CrystEngComm

PAPER

View Article Online
View Journal | View Issue

Cite this: *CrystEngComm*, 2015, **17**, 3023

Novel mixed 1D–2D lanthanide coordination polymers based on *p*-sulfonatocalix[4]arene and 4,4′-bipyridine-*N*,*N*′-dioxide where *p*-sulfonatocalix[4]arene acts as a guest†

Ahmad Husain and Clive L. Oliver*

Received 22nd January 2015,
Accepted 16th March 2015

DOI: 10.1039/c5ce00153f

www.rsc.org/crystengcomm

Two novel mixed 1D–2D coordination polymers based on 2D $[Ln(4,4'\text{-bpdo})_2(NO_3)_2(H_2O)_2]_n^+$ sheets and 1D $[Ln_2(4,4'\text{-bpdo})_2(C4AS)(NO_3)(H_2O)_9]_n$ chains (Ln = Sm for **1** and Ln = Nd for **2**) sustained by π···π interactions and lattice water facilitated hydrogen bonds have been established. The chains are arranged such that the *p*-sulfonatocalix[4]arene anions occupy the cavities of the 2D coordination polymer, and so act as guests rather than as hosts, which is their more usual role.

Introduction

Supramolecular chemistry of calixarenes offers a convenient approach to producing functional materials by directional and reversible non-covalent interactions,[1,2] with special attention to cation···π, C–H, and π···π interactions[3,4] including hydrogen bonds,[5,6] host–guest recognition,[1] donor–acceptor interactions,[7,8] and metal–ligand interactions.[9] Owing to the π-electron-rich hydrophobic cavity and the robust hydrophilic nature of the upper and lower rims,[10–12] calixarenes have drawn much attention in the burgeoning area of supramolecular chemistry[13] and coordination chemistry[14,15] due to its host enwrapping ability of small molecules and as a ligands, developing coordination complexes or polymers with various metal ions.[16–20] Specifically, *p*-sulfonatocalix[4]arenes with its pre-organized conical configuration and binding properties makes it an excellent model for molecular recognition and sensing, crystal engineering, catalysis, enzyme assays, and biological/medicinal chemistry.[6,21–24]Crowley and co-workers demonstrated that water-soluble *p*-sulfonatocalix[4]arene can bind lysine-rich cytochrome-c[25] and lysozyme,[26] forming a stable protein–calixarene complex, where *p*-sulfonatocalix[4]arene plays an important role in generating assemblies and promoting crystallization. Recently, Liu *et al.* also reported a supramolecular strategy to directly assemble the small molecular antipsychotic drug chlorpromazine into nanostructures, induced by *p*-sulfonatocalix[4]arene.[8] Liu and co-workers showed strong host–guest interaction between *p*-sulfonatocalix[4]arenes and a viologen that lead to a high degree of polymerization and viscosity.[27] Ling and co-workers established the self-assembly of *p*-sulfonatocalix[4]arene integrating various ionic liquid based symmetrical and unsymmetrical constituents in the presence of lanthanides and phosphonium cations.[28,29] A novel strategy for the construction of supramolecular assemblies have also been proposed by Liu *et al.* for the complexation with *p*-sulfonatocalix[*n*]arenes to promote the aggregation of aromatic or amphiphilic molecules by lowering the critical aggregation concentration, enhancing the aggregate stability, and regulating the degree of order in the aggregates.[30]

Since lanthanide ions have an extraordinary affinity for hard pyridyl-*N*-oxide donor groups, 4,4′-bipyridine-*N*,*N*′-dioxide (4,4′-bpdo) is an excellent candidate to construct 1D, 2D and 3D lanthanide metal coordination polymers. The relatively less sterically challenging nature, and orientation of the lone pairs on the pyridyl-*N*-oxide O atoms, results in a reasonably high flexibility apropos its coordination behaviour leading to structural diversity. Very recently, a channel supramolecular framework based on *p*-sulfonatocalix[4]arene nanocapsule using 4,4′-bipyridine-*N*,*N*′-dioxide and 2,2′-bipyridine-*N*,*N*′-dioxide together with Cu has been demonstrated by Zhang *et al.*[31] In this structure a 2D framework constructed from Cu and 4,4′-bipyridine-*N*,*N*′-dioxide acts as a host for *p*-sulfonatocalix[4]arene capsules. Zhang *et al.* also reported the guest inducing of *p*-sulfonatocalix[4]arene into three-dimensional capsule architecture based on terbium/europium(III) and pyrazine-*N*,*N*′-dioxide assembling in to mixed A–B double layered framework.[32] As part of our ongoing investigation of supramolecular assemblies based on the inclusion phenomena of *p*-sulfonatocalix[4]arene,[33] we

Centre for Supramolecular Chemistry Research, Department of Chemistry, University of Cape Town, Rondebosch, 7701, South Africa.
E-mail: Clive.Oliver@uct.ac.za; Fax: +27 21 6505195; Tel: +27 21 6503830

† Electronic supplementary information available: Crystal and geometrical data, structural depictions, TGA and DSC curves, PXRD patterns and an IR spectrum for **1**. CCDC reference numbers 1035921 and 1035922 for **1** and **2**, respectively. See DOI: 10.1039/c5ce00153f

report here a novel mixed 1D–2D network based on *p*-sulfonatocalix[4]arene and 4,4′-bipyridine-*N*,*N*′-dioxide with Sm(III) and Nd(III). As was the case in the Zhang *et al.*[31] structure the well-known host *p*-sulfonatocalix[4]arene acts as guest for a 2D coordination polymer, a reversal of its usual role.

Experimental section

Materials and physical measurements

All chemicals were of reagent grade, purchased from commercial sources, and used without further purification.

Hot-stage microscopy was performed on a Nikon SMZ-10 stereoscopic microscope fitted with a Linkam THMS600 hot stage and a Linkam TP92 control unit. Samples were placed under silicone oil on a cover slip and heated at 10 °C min^{-1}. Thermal events were monitored with a Sony Digital Hyper HAD colour video camera and captured using the Soft Imaging System program analysis.

Thermogravimetric analysis (TGA) measurements was performed at a heating rate of 10 °C min^{-1} in the temperature range 25–500 °C, under a dry nitrogen flow of 60 mL min^{-1} on a TGA Q500 instrument. About 3 mg of sample was placed in an open aluminium crucible.

Differential scanning calorimetry (DSC) measurement was performed at a heating rate of 10 °C min^{-1} in the temperature range 25–400 °C, under a dry nitrogen flow of 50 mL min^{-1} on a DSC Q200 instrument. About 2 mg of sample was placed in an aluminium pan with a lid. A sealed and empty pan was used as a reference.

Powder X-ray diffraction (PXRD) measurements were performed on a Bruker D8 Advance X-ray diffractometer in the 4–40° 2θ range using a 0.01° step size per second and X-rays generated at 30 kV and 40 mA.

Preparation of 1 as {[Sm(4,4′-bpdo)$_2$(NO$_3$)$_2$(H$_2$O)$_2$]$_n$}{[Sm$_2$(4,4′-bpdo)$_2$(C4AS)(NO$_3$)(H$_2$O)$_9$]$_n$}·4,4′-bpdo·NO$_3$·12H$_2$O

A mixture of Sm(NO$_3$)$_3$·6H$_2$O (44.5 mg, 0.1 mmol), pentasodium *p*-sulfonatocalix[4]arene (120 mg, 0.1 mmol) and 4,4′-bipyridine-*N*,*N*′-dioxide, (20 mg, 0.1 mmol) with a ratio of 1 : 1 : 1 (pH ~5) was dissolved in 3 ml hot water to yield a light yellow solution. Yellow block shaped crystals of compound **1** were obtained after volatilizing at 40 °C for a few days.

Preparation of 2 as {[Nd(4,4′-bpdo)$_2$(NO$_3$)$_2$(H$_2$O)$_2$]$_n$}{[Nd$_2$(4,4′-bpdo)$_2$(C4AS)(NO$_3$)(H$_2$O)$_9$]$_n$}·4,4′-bpdo·NO$_3$·12H$_2$O

Compound **2** was obtained by similar procedure as for **1** except that Nd(NO$_3$)$_3$·6H$_2$O was used instead of samarium nitrate.

Single crystal X-ray diffraction analysis and structure determination

Suitable, apparently single crystals of **1** and **2** were selected and mounted on a cryoloop in oil. Data collection was carried out on a Bruker DUO APEX II CCD diffractometer using graphite monochromated Mo Kα (λ = 0.71073 Å) radiation with the crystal cooled to 100(2) K using an Oxford Cryostream-700. CELL_NOW identified **1** and **2** as 3- and 2-component non-merohedral twins, respectively.[27] Data reduction and cell refinement were performed using SAINT-Plus.[34] The X-ray diffraction data were corrected for Lorentz-polarization factor and scaled for absorption effects by using TWINABS.[35] The structure was solved by direct methods, implemented in SHELXS-97.[36] Refinement procedure by full-matrix least-squares method, based on F^2 values against all reflections was performed by SHELXL-2014/7 using an 'HKLF 5' data format incorporating the data from all the twin domains,[35] including anisotropic displacement parameters for all non-H atoms. The twin domains refined to values of (0.654(2), 0.1987(16), 0.1469(15)) for **1** and to (0.5075(6), 0.4925(6)) for **2**, respectively. Although we were not able to locate all the hydrogen atoms for the disordered lattice water molecules, the contribution of hydrogen atoms are included in the SFAC instruction in the SHELXL-2014/7 refinement.

CCDC 1035921 and 1035922 contains the supplementary crystallographic data for this paper.

Results and discussion

Compound **1** and **2** crystallized from a hot aqueous solution of pentasodium *p*-sulfonatocalix[4]arene (Na_5C4AS) salt, 4,4′-bipyridine-*N*,*N*′-dioxide (4,4′-bpdo) and metal (Sm (**1**) and Nd(**2**)) nitrate hexahydrate (Scheme 1).

Single crystal X-ray structure analyses reveal that complexes **1** and **2** are isostructural and crystallize in centrosymmetric space group $P\bar{1}$, so **1** was chosen to represent the structural discussion. Crystallographic data are listed in Table 1.

The asymmetric unit consist of two crystallographically independent coordination complex components (Fig. 1), one lattice 4,4′-bipyridine-*N*,*N*′-dioxide molecule, one lattice nitrate anion and twelve lattice water molecules. Component one, [Sm$_2$(4,4′-bpdo)$_2$(C4AS)(NO$_3$)(H$_2$O)$_9$] is composed of one *p*-sulfonatocalix[4]arene moiety, one and two half 4,4′-bpdo molecules bridging Sm2 and Sm3 and so forms a zigzag 1-dimensional polymeric chain in the extended structure which propagates along the [$\bar{1}$02] direction. Component two, [Sm(4,4′-bpdo)$_2$(NO$_3$)$_2$(H$_2$O)$_2$]$^+$ is composed of Sm1 bonded to four half (bridging) 4,4′-bpdo ligands along with two nitrate anions in a bidentate coordination fashion, forming a 2-dimensional layer in the extended structure. The rest of the coordination sphere for the Sm1 cation is completed by two aqua ligands. All four 4,4′-bpdo ligands responsible for extending the 2D network are situated about inversion centres.

All the three crystallographically unique Sm(III) cations display different coordination geometries. The skeletal

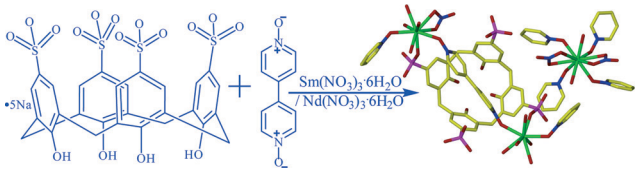

Scheme 1 Preparation of compound **1** and **2**.

Table 1 Crystal data and structure refinement for **1** and **2**

Empirical formula	$C_{78}H_{105}N_{14}O_{61}S_4Sm_3$ (1)	$C_{78}H_{105}N_{14}O_{61}S_4Nd_3$ (2)
Formula weight	2793.95	2774.61
Temperature (K)	173(2)	173(2)
λ (Å)	0.71073	0.71073
Crystal system	Triclinic	Triclinic
Space group	$P\bar{1}$	$P\bar{1}$
Unit cell dimensions (Å), (°)	a = 15.9282(12), α = 116.84(2) b = 18.6918(15), β = 91.34(2) c = 19.2219(15), γ = 90.92(2)	a = 15.9870(15), α = 116.97(2) b = 18.7220(18), β = 91.38(2) c = 19.3040(19), γ = 90.88(2)
Volume (Å^3)	5102.3(7)	5145.7(9)
Z	2	2
ρ (g cm^{-3})	1.810	1.783
μ (mm^{-1})	1.903	1.688
F_{000}	2792	2780
Crystal size (mm^3)	0.55 × 0.24 × 0.20	0.52 × 0.27 × 0.12
θ (°)	1.18–27.00	1.18–28.44
Miller index ranges	$-20 \le h \le 20$, $-23 \le k \le 21$, $0 \le l \le 24$	$-21 \le h \le 21$, $-25 \le k \le 22$, $0 \le l \le 25$
Reflections collected	52 697	25 582
Independent reflections	39 868	25 582
Completeness to θ_{max} (%)	100	100
Refinement method	Full-matrix least-squares on F^2	Full-matrix least-squares on F^2
Data/restraints/parameters	39 868/1336/1519	25 582/1283/1503
Goodness-of-fit on F^2	1.053	1.033
Final R indices [$I > 2\sigma(I)$]	R_1 = 0.0372, wR_2 = 0.1070	R_1 = 0.0471, wR_2 = 0.1034
R indices (all data)	R_1 = 0.0416, wR_2 = 0.1101	R_1 = 0.0737, wR_2 = 0.1142
Largest diff. peak and hole (e Å^{-3})	1.229 and −0.979	1.291 and −0.882

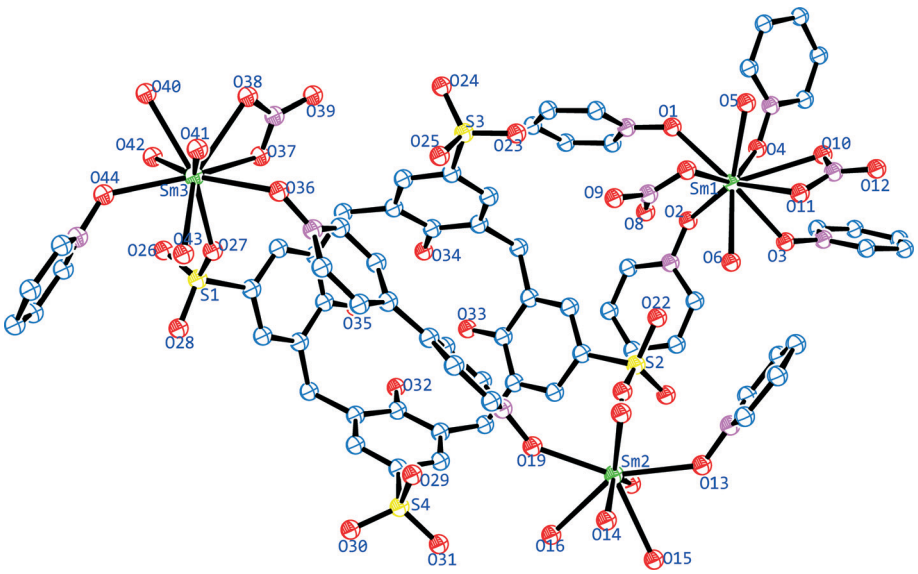

Fig. 1 Ortep diagram of **1**, showing atomic displacement parameters (ellipsoids drawn at the 50% probability level). Hydrogen atoms, solvent water molecules, lattice 4,4′-bpdo molecule and the nitrate anion were omitted. Only atoms pertinent to the structural description have been labelled for the sake of clarity.

structure around Sm1 is a distorted bicapped square antiprism (Fig. 2a) with the O8 and O10 atoms from the nitrate anions at the bicapped positions, with the bond angle O10–Sm1–O8 being 160.42(10)°, which are at relatively longer distances (Tables S1 & S2†) than other O atoms from the Sm1 cation. The Sm2 cation is eight coordinated in a square antiprismatic fashion by eight O atoms (Fig. 2b) in which the set of atoms O16, O17, O19, O20 with a torsion angle of 12.76° and the set of atom O13, O14, O15, O18 with a torsion angle of 24.75° form two approximate square (top and bottom) planes, which are almost parallel to each other. The nine-coordinate Sm3 cation adopts a monocapped square antiprismatic geometry (Fig. 2c), having O37 from a ligated nitrate anion at the capped position. The Sm–O bond distances are in the 2.304(3)–2.675(3) Å range, which compares well with literature values.[31,32,37,38] Selected bond lengths and bond angles are given in Tables S1 & S2.†

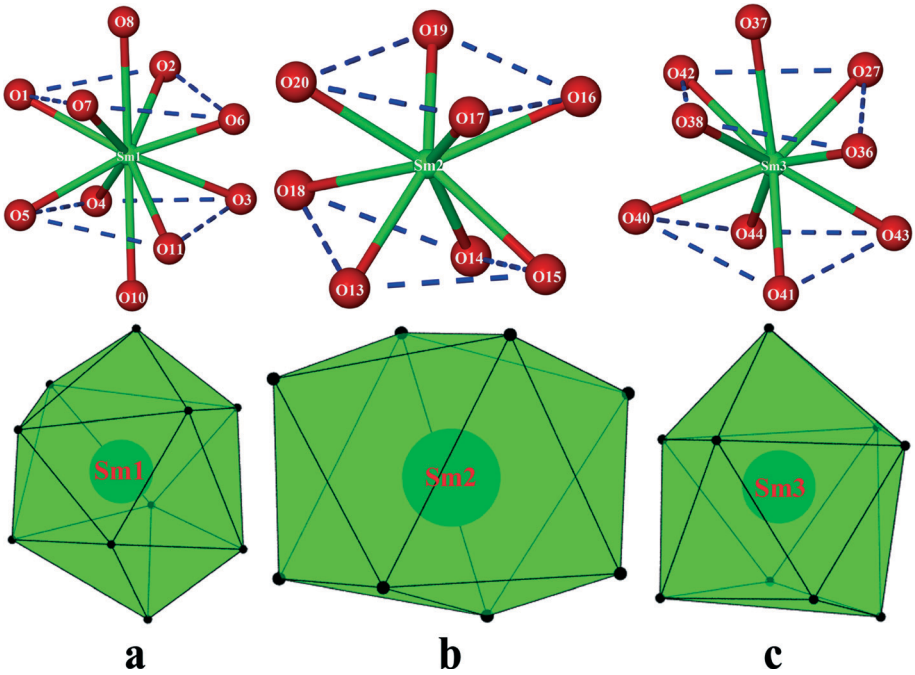

Fig. 2 Display of Sm(III) coordination environment. (a) For Sm1, (b) for Sm2 and (c) for Sm3.

The Sm1 cation and four half 4,4′-bipyridine-*N*,*N*′-dioxide ligands form a 2D layered network based on a (4, 4) topology exhibiting bowl-shaped cavities which encapsulate the *p*-sulfonatocalix[4]arene anions (Fig. 3b). This is similar to the Zhang *et al.* structure,[31] except that in this case neighbouring *p*-sulfonatocalix[4]arene entities, form a 1D polymer *via* coordination bonds. Even though the *p*-sulfonatocalix[4]arene is a ligand in forming the 1D polymer we take the view that ligation does not preclude the interaction between the 1D polymer and the 2D polymer from being described as a host–guest interaction where the 2D polymer forms the host cavity and *p*-sulfonatocalix[4]arene is the guest entity.[39–41] In the crystal structure, the four Sm atoms and four 4,4′-bpdo ligands build up a bevel square shaped cavity with Sm⋯Sm distances of 13.410 and 13.668 Å. The torsion angles between the planes formed by opposite 4,4′-bpdo ligands of this framework are 31.40° and 65.57° while the torsion angle between the planes of the adjacent Sm atoms is 42.44° providing conical shape cavity. Similar motifs based on 4,4′-bpdo and 2,2′-bpdo with Cu(II) have also been observed by Zhang *et al.*,[31] however this arrangement is completely different from that of Zhang *et al.* All four Cu atoms in the Zhang *et al.*[31] motifs were almost co-planar with the O–Cu–O angle of 165 and 179.3°, whilst in our case the four metal ions are not co-planar with the O–Sm–O angles being 142.8° and 73.4°, probably to accommodate the coordinated nitrate anion in coordination sphere that finally lead to a conical cavity. This is further responsible for the slantwise long range weak π⋯π interactions.

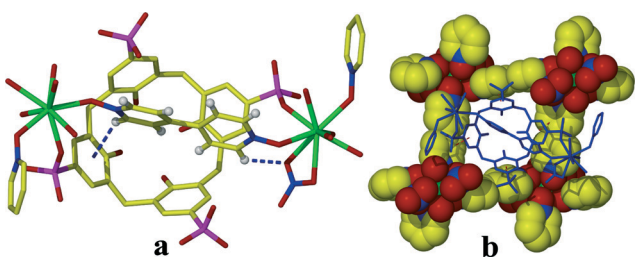

Fig. 3 (a) 4,4′-bpdo 'perched' in the cavity of C4AS *via* C–H⋯π and C–H⋯O interactions. (b) C4AS residing in the cavity formed by $[Sm(4,4'\text{-bpdo})_2(NO_3)_2(H_2O)_2]^+$.

At the upper rim of C4AS, one 4,4′-bipyridine-*N*,*N*′-dioxide ligand is 'perched', the two pyridine rings twisted at an angle of 21.23°, since the cavity is too small to support lateral encapsulation of 4,4′-bpdo (Fig. 3a) which is transversely orientated with the N–O groups directed towards two opposing sulfonate groups of the C4AS. Both groups bridge the Sm2 and Sm3 cations.

There are non-classical hydrogen bonding interactions between the 4,4′-bpdo and the *p*-sulfonatocalix[4]arene, with the closest C–H⋯aromatic centroid distance of 3.290 Å in **1** (3.302 Å in **2**). The *p*-sulfonatocalix[4]arene anion is present in its usual flattened cone conformation with C_{2v} symmetry (cone angles between the planes of opposite aromatic rings are 65.18° and 82.28°). Accordingly, the largest angles between the planes of aromatic rings and the plane of the phenolic oxygen atoms are 133.53° in **1** (133.78° in **2**).

At pH ~5 *p*-sulfonatocalix[4]arene takes on an overall charge of −5, with two of the opposing sulfonate groups bonded to two Sm(III) cations. There are four nitrate anions which results in a total negative charge of −9 to balance with the three Sm(III) cations. It was not possible to locate all hydrogen atoms for disordered water molecules from the

difference Fourier map as there was not enough electron density. Two Sm(III) ions connected by two bridging 4,4′-bpdo in a *trans* fashion and sulfonate group from C4AS form 1D chains which pack together in the crystal lattice to form infinite double stranded regular zigzag chains running along the *c*-axis (Fig. 4b). Each zigzag chain has a repeating motif of length of 42.14 Å (Fig. 4a). The interplay between chains is governed by 4,4′-bpdo···4,4′-bpdo transversely π-stacking interactions *via* lattice 4,4′-bpdo (centroid···centroid distance 3.95–4.25 Å), such that a 2D network of chains propagating along *ac*-plane is obtained throughout the crystal lattice this sheet structure is further sandwiched between the 2D sheets comprised of $[Sm(4,4'\text{-bpdo})_2(NO_3)_2(H_2O)_2]^+$.

In the $[Sm(4,4'\text{-bpdo})_2(NO_3)_2(H_2O)_2]^+$ 2D-sheets, four Sm(III) ions connected by four bridging 4,4′-bpdo ligands define the main skeleton of the 2D sheets (Fig. 4c and Fig. S1†) stacked together parallel to *ac*-plane. Adjacent sheets are linked together *via* the 1D chain through intermolecular hydrogen bonds and π···π-stacking interactions. The Sm–O distances for 4,4′-bpdo (2.25–2.39 Å) are shorter than those for C4AS (2.46–2.52 Å). The usual "up–down" relative arrangement of neighbouring *p*-sulfonatocalix[4]arene anions which is exhibited in the vast majority of structures containing this anion, is retained since the 4,4′-bdpo ligands of the 2D network simply act as spacers.

The lattice 4,4′-bpdo interacts with the 4,4′-bpdo ligated to Sm2 and Sm3 *via* π···π interaction (3.874–4.218 Å) to form two-dimensional sheets by joining the 1D chains of C4AS through the plane formed by these 4,4′-bpdo ligands as depicted in Fig. S2.†

Within the zigzag chain O25 from the sulfonate group in bifurcated mode interacts with H41a and H43a of the water molecules bonded to Sm3 *via* strong hydrogen bonds forming a six membered synthon of $R_2^1(6)$ type (Fig. 5). Two strands also interact *via* strong hydrogen bond O14–H14a···O29 ($d_{H\cdots A}$ = 1.85 Å, $d_{D\cdots A}$ = 2.706(4) Å, ∠D–H···A = 167.8°, $-x+2, -y+1, -z+1$) forming a slantwise capsular structure where both up–up facing C4AS from opposite strands are completely offset to each other. H16a of the water molecule bonded to Sm2 interact with O39 ($d_{H\cdots A}$ = 2.03 Å) *via* a strong hydrogen bond (Tables S3 & S4†). 'The double strand zigzag chain interacts with the neighbouring parallel chain *via* these hydrogen bonds extending the network in the [100] direction. There is no direct hydrogen bonding interaction between the 1D chain network and 2D network within the lattice. However they interact *via* lattice water mediated hydrogen bonding. They also interact *via* π···π (centroid···centroid 3.969–4.290 Å) interaction between the C4AS aryl rings and the pyridyl rings of the 4,4′-bpdo ligand of 2D network. The O46 atom of the lattice 4,4′-bpdo is hydrogen bonded ($d_{H\cdots A}$ = 1.93 Å, $d_{D\cdots A}$ = 2.669(4) Å,

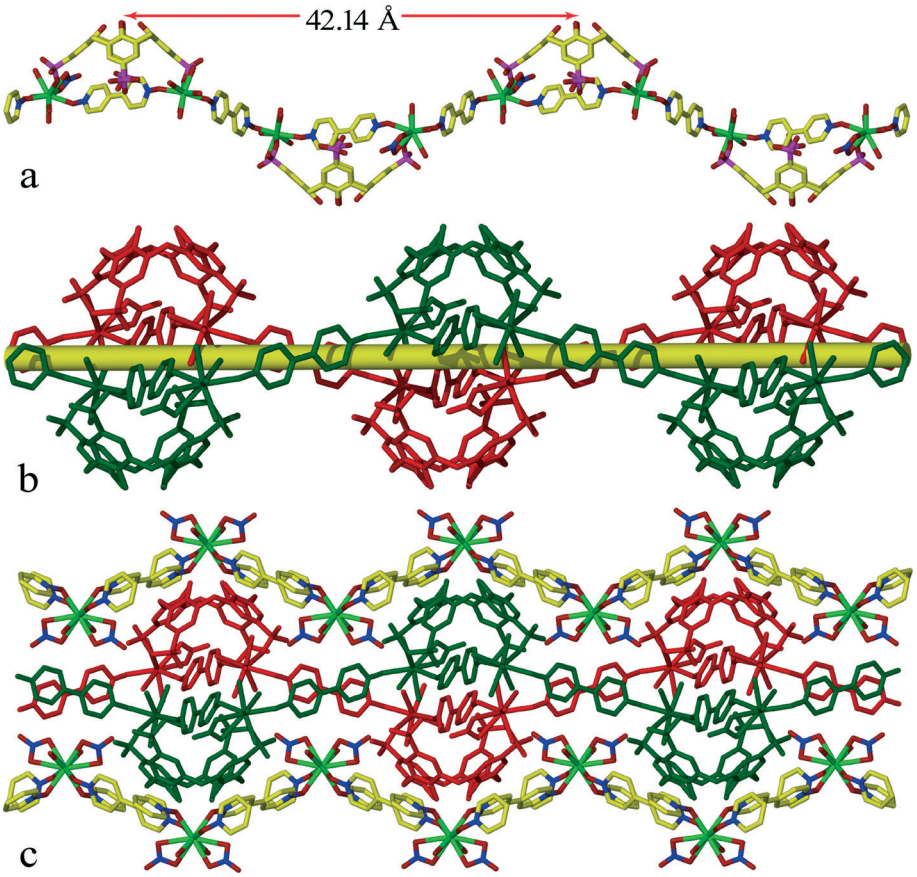

Fig. 4 (a) A view of one zigzag strand in **1** (viewed down the *a*-axis) highlighting the repeat distance of the zigzag chain. (b) A representation of two chains propagating along the *c*-axis. (c) Sandwiched twisted 1-D chains located between the 2D sheets.

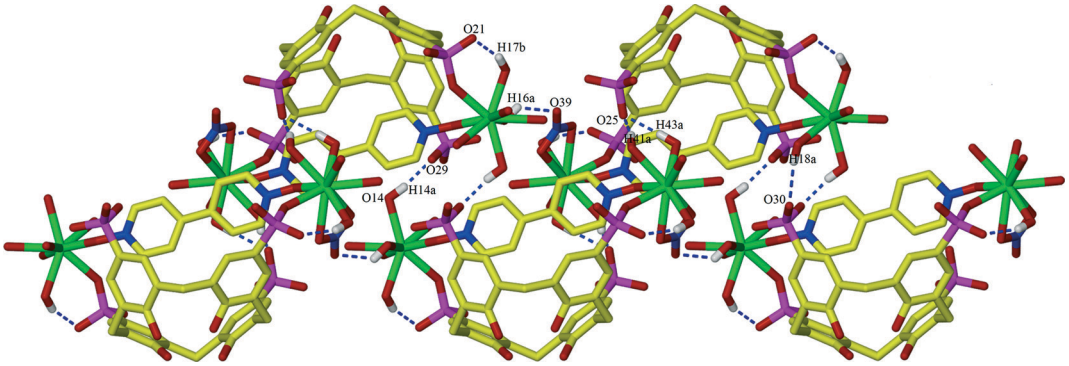

Fig. 5 Display of H-bonding between the 1D chains. H atoms (except for those involving hydrogen bonding) have been omitted for clarity.

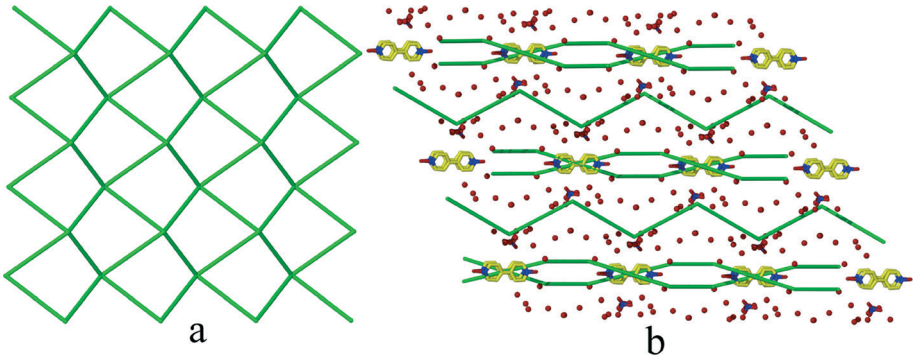

Fig. 6 Display of 4-connected uninodal nets viewed down the (a) *b*-axis, (b) Schematic display of double zigzag 1D chains along with lattice water and 4,4′-bpdo molecules sandwiched between 2D sheets as viewed down the *c*-axis.

∠D–H···A = 146.9°, $-x + 1$, $-y + 1$, $-z + 1$) to the water hydrogen atoms of Sm3 forming an eight membered R_3^2 (8) synthon mediated by lattice water O56. Interestingly, the extended structure of complex **1** and **2** shows infinitely extended hydrated channels running through [001] direction (Fig. S3†).

Powder X-ray diffraction (PXRD) patterns are provided in the ESI† for **1** and **2** (Fig. S6†). In both cases, the experimental patterns agree well with the calculated patterns. This indicates that the structure of the bulk material matches the single crystal X-ray structure for both **1** and **2**. The experimental PXRD pattern of **2** does exhibit an 'extra' peak at ~6.5° 2θ, which may indicate the presence of a small impurity (*e.g.* a small amount of unreacted material), however, the rest of the pattern agrees well with the calculated PXRD pattern.

Topological studies

Sm(3) centre of $[Sm(4,4'\text{-bpdo})_2(NO_3)_2(H_2O)_2]^+$ serves as a 4-connected node by linking to four 4,4-bipyridine-*N*,*N*-dioxide (4,4′-bpdo) ligands with the vertex symbol of [4.4.4.4.6(2).6(2)] to generate a 2-D sheet parallel to the *ac*-plane. Thus, a 2D (4)-connected network with the Schally symbol of {4^4·6^2}–VS[4·4·4·4·*·*] is generated with *4-c uninodal*[42] *sql*/Shubnikov topology as depicted in Fig. 6.

Thermal analysis

The TG data of complex **1** indicates two mass losses (Fig. S4†). The first mass loss 50–140 °C (8.464%) corresponds to the loss of all the lattice water molecules

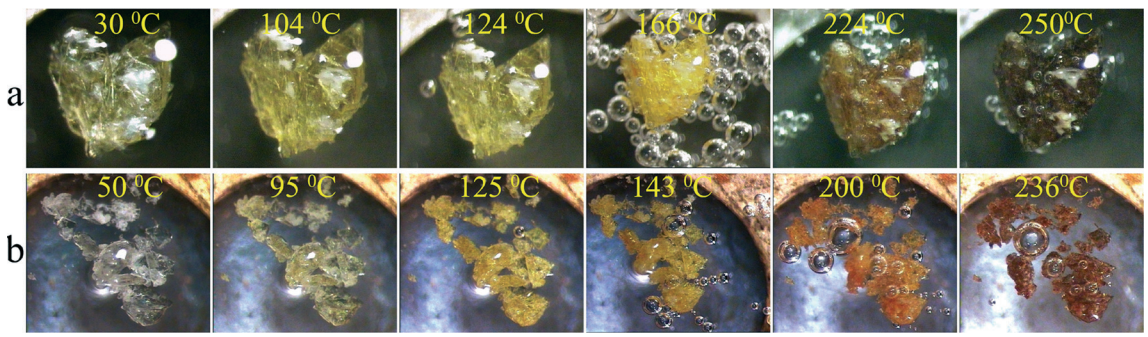

Fig. 7 Hot stage microscope photograph of compounds **1** (a) and **2** (b) to showing the release of solvent at various temperatures. The crystals were immersed in silicone oil to indicate the release of solvent molecules.

(calculated: 8.42%). A long range mass loss in the range 150–500 °C (20%) corresponds to the loss of all the coordinated water molecules along with the nitrate ion, subsequently followed by structural decomposition. DSC shows one broad endotherm peak which should be due to the loss of solvent molecules (Fig. S4†) and one broad exotherm due to structural decomposition. Hot stage microscopy indicates visual loss of water occurs for **1** and **2** at various temperatures (Fig. 7). The presence of lattice water molecules was also confirmed by the presence of broad peak at ~3400–3600 cm^{-1} IR spectrum (Fig. S5†).

Conclusion

In summary, this work describes two isostructural mixed 1D–2D coordination polymers. In each case the structures are comprised of two components – a two-dimensional 4-connected framework made up of Sm/Nd nitrate centres bridged by 4,4′-bipyridine-*N*,*N*′-dioxide ligands and a one-dimensional chains of Sm/Nd nitrate centres bridged by 4,4′-bipyridine-*N*,*N*′-dioxide ligands and *p*-sulfonatocalix[4]arene ligands. Both supramolecular assemblies have been carefully studied from viewpoints of both complexation mode and extended structure. Interestingly, the well-known host molecule *p*-sulfonatocalix[4]arene, as part of the 1D polymer, acts as a guest for the 2D framework similar to the case of the Zhang *et al.* structure. Our present work provides 2 isostructural examples which show that this rare class of compounds can be extended. Moreover, it represents an advance in the complexity of these structures by way of the 1D polymerization of the *p*-sulfonatocalix[4]arene component with the retention of the hydrated channels. This may ultimately affect its porous properties and thus the present study contributes to the investigation of suitable manipulation factors in the pursuit of constructing functional solid-state materials in supramolecular chemistry and crystal engineering.

Acknowledgements

A.H. and C.L.O. thanks the South African National Research Foundation and the University of Cape Town for financial support.

References

1 X. Ma and H. Tian, *Acc. Chem. Res.*, 2014, **47**, 1971–1981.
2 O. Danylyuk and K. Suwinska, *Chem. Commun.*, 2009, 5799–5813.
3 K. D. Daze and F. Hof, *Acc. Chem. Res.*, 2013, **46**, 937–945.
4 V. Francisco, N. Basílio and L. García-Río, *J. Phys. Chem. B*, 2014, **118**, 4710–4716.
5 M. E. Belowich, C. Valente, R. A. Smaldone, D. C. Friedman, J. Thiel, L. Cronin and J. F. Stoddart, *J. Am. Chem. Soc.*, 2012, **134**, 5243–5261.
6 O. Danylyuk, H. Butkiewicz, A. W. Coleman and K. Suwinska, *CrystEngComm*, 2015, **17**, 1745–1749.
7 S. J. Dalgarno, M. J. Hardie, M. Makha and C. L. Raston, *Chem. – Eur. J.*, 2003, **9**, 2834–2839.
8 Z. Qin, D.-S. Guo, X.-N. Gao and Y. Liu, *Soft Matter*, 2014, **10**, 2253–2263.
9 Y. Liu, Z. Huang, X. Tan, Z. Wang and X. Zhang, *Chem. Commun.*, 2013, **49**, 5766–5768.
10 T. Schrader, *Nat. Chem.*, 2012, **4**, 519–520.
11 P. Muthu Mareeswaran, E. Babu, V. Sathish, B. Kim, S. I. Woo and S. Rajagopal, *New J. Chem.*, 2014, **38**, 1336–1345.
12 S. M. Taylor, R. D. McIntosh, S. Piligkos, S. J. Dalgarno and E. K. Brechin, *Chem. Commun.*, 2012, **48**, 11190–11192.
13 R. Sun, C. Xue, M. Gao, H. Tian and Q. Li, *J. Am. Chem. Soc.*, 2013, **135**, 5990–5993.
14 J. Li, S. Zhang, Y.-G. Chen, X. Du, H. Yu and J. Yu, *Inorg. Chem. Commun.*, 2014, **47**, 93–95.
15 M. Liu, W. Liao, C. Hu, S. Du and H. Zhang, *Angew. Chem., Int. Ed.*, 2012, **51**, 1585–1588.
16 R. Mclellan, M. A. Palacios, C. M. Beavers, S. J. Teat, S. Piligkos, E. K. Brechin and S. J. Dalgarno, *Chem. – Eur. J.*, 2015, **21**, 1–10.
17 N. Mattoussi, G. Pilet, G. Novitchi, F. Meganem and D. Luneau, *Eur. J. Inorg. Chem.*, 2013, 2652–2656.
18 F. Gándara, E. Gutiérrez-Puebla, M. Iglesias, N. Snejko and M. A. Monge, *Cryst. Growth Des.*, 2010, **10**, 128–134.
19 Y. Bi, W. Liao, G. Xu, R. Deng, M. Wang, Z. Wu, S. Gao and H. Zhang, *Inorg. Chem.*, 2010, **49**, 7735–7740.
20 Y. Bi, X. T. Wang, W. Liao, X. Wang, R. Deng, H. Zhang and S. Gao, *Inorg. Chem.*, 2009, **48**, 11743–11747.
21 F. Perret and A. W. Coleman, *Chem. Commun.*, 2011, **47**, 7303–7319.
22 J. L. Atwood, L. J. Barbour, M. J. Hardie and C. L. Raston, *Coord. Chem. Rev.*, 2001, **222**, 3–32.
23 D.-S. Guo and Y. Liu, *Chem. Soc. Rev.*, 2012, **41**, 5907–5921.
24 K. Wang and Y.-W. Yang, *Annu. Rep. Prog. Chem., Sect. B: Org. Chem.*, 2013, **109**, 67–87.
25 R. E. McGovern, H. Fernandes, A. R. Khan, N. P. Power and P. B. Crowley, *Nat. Chem.*, 2012, **4**, 527–533.
26 R. E. McGovern, A. A. McCarthy and P. B. Crowley, *Chem. Commun.*, 2014, **50**, 10412–10415.
27 K.-P. Wang, D.-S. Guo, H.-X. Zhao and Y. Liu, *Chem. – Eur. J.*, 2014, **20**, 4023–4031.
28 I. Ling, B. W. Skelton, A. N. Sobolev, Y. Alias and C. L. Raston, *CrystEngComm*, 2014, **16**, 5159–5164.
29 I. Ling, Y. Alias and C. L. Raston, *New J. Chem.*, 2010, **34**, 1802–1811.
30 B. Jiang, D. Guo, Y. Liu, K. Wang and Y. Liu, *ACS Nano*, 2014, **8**, 1609–1618.
31 G.-L. Zheng, G.-C. Yang, S.-Y. Song, X.-Z. Song and H. Zhang, *CrystEngComm*, 2014, **16**, 64–68.
32 G. Zheng, F. Zhang, Y. Li and H. Zhang, *CrystEngComm*, 2008, **10**, 1560–1564.
33 A. Husain and C. L. Oliver, *CrystEngComm*, 2014, **16**, 3749–3757.
34 *Bruker (2007)*, Bruker AXS Inc., Madison, Wisconsin USA, 2007.

35 G. M. Sheldrick, *TWINABS*, Bruker AXS Inc., Madison, Wisconsin USA, 2001.
36 G. M. Sheldrick, *Acta Crystallogr., Sect. A: Found. Crystallogr.*, 2008, **64**, 112–122.
37 A. V. Pavlishchuk, S. V. Kolotilov, I. O. Fritsky, M. Zeller, A. W. Addison and A. D. Hunter, *Acta Crystallogr., Sect. C: Cryst. Struct. Commun.*, 2011, **67**, m255–m265.
38 G. J. Palenik, *Inorg. Chem.*, 2003, **42**, 2725–2728.
39 K. Xiong, M. Wu, Q. Zhang, W. Wei, M. Yang, F. Jiang and M. Hong, *Chem. Commun.*, 2009, 1840–1842.
40 S. J. Dalgarno, J. L. Atwood and C. L. Raston, *Cryst. Growth Des.*, 2006, **6**, 174–180.
41 G. Zheng, H.-J. Zhang, S.-Y. Song, Y.-Y. Li and H.-D. Guo, *Eur. J. Inorg. Chem.*, 2008, 1756–1759.
42 L. Qin, J. Zheng, S.-L. Xiao, X.-H. Zheng and G.-H. Cui, *Inorg. Chem. Commun.*, 2013, **34**, 71–74.